ELECTROMAGNETIC INVESTIGATION OF THE RESISTIVITY STRUCTURES AROUND AND BENEATH THE EYJAFJALLAJÖKULL VOLCANO, SOUTHERN ICELAND: PRELIMINARY RESULTS

Marion P. Miensopust[1,2], Alan G. Jones[1], Gylfi P. Hersir[3] and Arnar M. Vilhjálmsson[3]

[1] Dublin Institute for Advanced Studies, School of Cosmic Physics, Dublin, Ireland
[2] Institut für Geophysik, Westfälische Wilhelms-Universität Münster, Germany
[3] Iceland GeoSurvey, Reykjavík, Iceland

ABSTRACT - Due to the recent eruptive and highly disruptive volcanic events in 2010 in Iceland, scientific and societal interest is overwhelming in gaining as much information as possible about the volcanic structures and processes to enhance the understanding of the partially glacier-covered Eyjafjallajökull and Katla volcanic systems. Numerous petrological, geochemical and geophysical investigations of these systems have already been published. However, to date no electrical or electromagnetic data have been acquired on these two volcanoes to attempt to image the resistivity structure beneath and around them, although electromagnetic methods are far more sensitive to fluid distribution (in this case partial melt) than any other geophysical method.
In July 2011, a pilot study took place to collect broadband magnetotelluric (MT) data around the Eyjafjallajökull. The MT data are supplemented with transient electromagnetic (TEM) measurements. This data set is the first one collected at these volcanic systems and will complement the existing geophysical data. Very fresh data and preliminary results from the experiment will be shown.

INTRODUCTION

Iceland has numerous active volcanoes, some of which are covered by glaciers. The Eyjafjallajökull volcano in southern Iceland has an ice-capped crater and its 'sister volcano', Katla, that erupted twice in historic times (within the last 1,100 years) synchronously with the Eyjafjallajökull, is mostly covered by a glacier. The volcanic system of Katla is one of the most active ones in Iceland with at least twenty eruptions within the central volcano and one in its fissure swarm during the past 1,100 years (Larsen, 2000). These eruptions have been quite regularly twice every century, but the last eruption in 1918 is almost 100 years ago. The volcano is mostly covered by the Mýrdalsjökull ice cap and, therefore, eruptions within the Katla volcano are phreato-magmatic in type and are capable of producing jökulhlaups (or glacier bursts), i.e., sudden glacial outburst floods (Sturkell et al., 2010). The neighbouring volcano, 25 km to the west, is Eyjafjallajökull, which is covered by a smaller and thinner glacier. It is less active than Katla with the most recent (in March/April 2010) and two historic eruptions recorded during the last 1,100 years. These two known historic events occurred in tandem, the first simultaneously with the Katla eruption of 1612, and the second being the eruption in 1821-1823 that was immediately followed by an eruption of Katla (Sturkell et al., 2010 and references therein in Icelandic). Both volcanoes are in proximity to populated areas and to international flight paths, which makes them both potent societal threats, although the erupted volume of Katla has been orders of magnitude larger than those of Eyjafjallajökull. The recent eruptive events of the Eyjafjallajökull volcano have focused major public interest - even more than ever before - on volcanic eruptions (not only on their local effects but also on potential long-distant effects on daily life). Scientific interest is

overwhelming in gaining as much information as possible about the volcanic structures and processes to enhance understanding. Based on the historic eruptive connections between these two volcanoes, there is the apprehension that the 2010 eruption of Eyjafjallajökull will be followed by a larger eruption of Katla. Therefore, interest in knowing the volcanic structures of both volcanoes and understanding the possible links between them is heightened.

Beside numerous petrological and geochemical studies also some geophysical investigations on the Eyjafjallajökull and Katla volcanoes have been published showing results from GPS measurements (e.g., Árnadóttir et al., 2008), earthquake studies (e.g., Dahm & Brandsdóttir, 1997; Einarsson & Brandsdóttir, 2000), radar altimetry and interferometry (e.g., Guðmundsson et al., 2007; Hooper et al., 2009), seismic surveys (e.g., Guðmundsson et al., 1994), and aeromagnetic measurements (e.g., Jónsson & Kristjánsson, 2000). The bedrock surface of Mýrdalsjökull has been mapped by radio echo soundings (Björnsson et al., 2000). Recently Sigmundsson et al. (2010) outline their understanding of the intrusive processes based on GPS measurements, interferometric analysis of satellite radar images and seismic data recorded over several months before and during the 2010 eruptive events. However, to date no electric or electromagnetic (EM) methods have been applied to attempt imaging the resistivity structure beneath and around these two volcanoes, although EM methods are far more sensitive to fluid distribution (in this case partial melt) than any other geophysical method. Therefore, the aim of the project conducted by Iceland GeoSurvey (ISOR) and Dublin Institute for Advanced Studies (DIAS) is to investigate the resistivity structure beneath and around the Eyjafjallajökull using the magnetotelluric (MT) and transient electromagnetic (TEM) methods.

DATA COLLECTION AND PROCESSING

In July 2011, broadband MT data were collected at 26 sites around the Eyjafjallajökull and the southern part of Mýrdalsjökull (Figure 1) using MTU5/MTU5A systems from Phoenix Geophysics. Both horizontal electric field components were recorded using 100 m dipoles, and the vertical and both horizontal magnetic field components were measured using induction coils. At most sites the recording time was approximately 40 hours, and a distant remote reference site (about 150 km away) was recording during the whole survey. The obtained period range of good quality data is about 0.003 to 1,000 – 2,000 s. In addition, at 25 of the MT sites central loop TEM data were obtained using a transmitter loop of 200 m x 200 m and a 1 m^2 receiver loop with 100 windings (effective area 100 m^2).

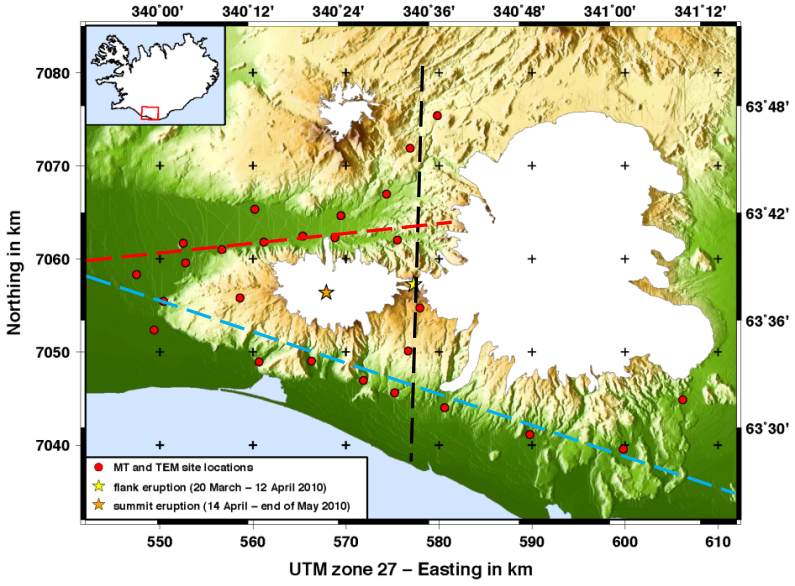

Figure 1: Map showing the locations of the 26 MT and TEM sites, flank and summit eruption sites as well as dashed lines indicating the position of cross-sections shown in Figure .

Phoenix commercial remote-reference processing software (based on Jones and Jödicke (1984)/method 6 in Jones et al. (1989)) was used to convert the time series of the magnetotelluric data into transfer functions. To obtain the best response curves combinations of electric field and magnetic field references as well as a far remote (remote reference site about 150 km away from array) and a local remote (array site that recorded at the same time) were investigated. For many sites an electric field remote reference resulted in better estimates for short periods whereas a magnetic field remote reference produced better results for long periods. Figure 2 shows apparent resistivity and phase curves as well as induction arrows using Wiese convention (Wiese, 1962) for an example site. The transfer functions were merged from electric field remote reference estimates for periods < 10 s and magnetic field remote reference estimates > 10 s. In general, the data quality is very good and the transfer functions suggest at least for the first three decades a 1D structure.

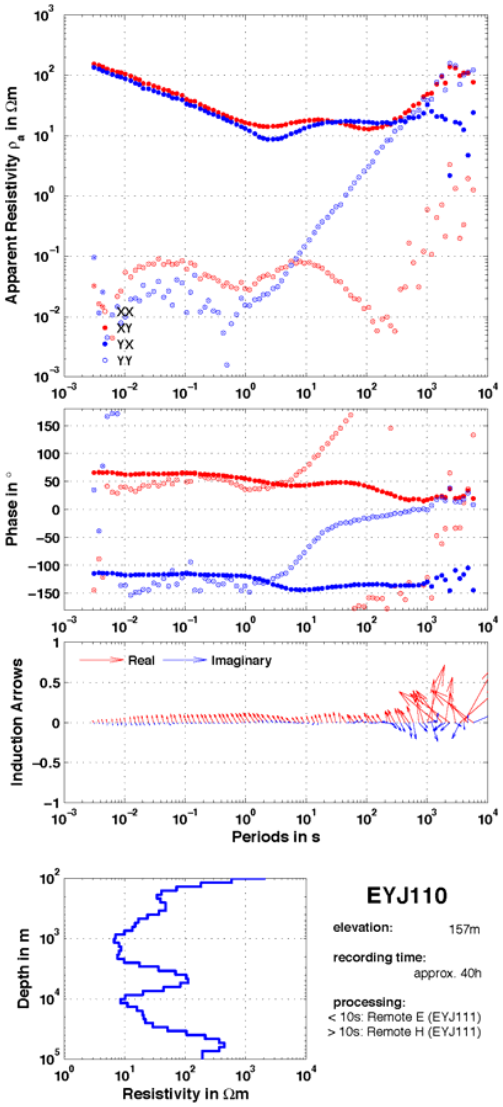

Figure 2: Response curves of an example site. Apparent resistivity curves (top), phase curves (middle) and induction arrows (bottom) in Wiese convention (Wiese, 1962) are shown. Below are information about this particular site and the obtained 1D Occam model of the invariants.

PRELIMINARY RESULTS

Small-scale, near-surface resistivity heterogeneities and topography can affect MT responses. This phenomenon is known as distortion. If the distortion is purely galvanic (as assumed for the MT case), the phase relationship between the horizontal electric and magnetic field vectors will be virtually unaffected and only the amplitudes of the observed electric field are distorted. Taken advantage of this, Caldwell et al. (2004) introduced the phase tensor approach. The graphical representation of the phase tensor is an ellipse. The principle axes of the phase tensor ellipse (ϕ_{max}, ϕ_{min}) indicate the horizontal directions of the maximum and minimum induction current, which reflects lateral variations in the resistivity structure. The phase tensor skew angle (β), and the variation of the direction of the major axis of the phase tensor ellipse can help in determining the dimensionality of the structure. In the case of an isotropic, 1D structure, $\phi_{max} = \phi_{min}$ and therefore the phase tensor will be represented by circles. In the 2D case, $\phi_{max} \neq \phi_{min}$ and the phase tensor is represented by an ellipse. For the 1D and 2D case, the phase tensor is symmetric (theoretically: $\beta = 0$), whereas for the 3D case the phase tensor is not symmetric and accordingly the skew angle will be non-zero. Figure 3 shows phase tensor maps including induction arrows for 0.5 km, 1.5 km and 7.5 km depth below surface (Niblett-Bostick penetration depth estimation). The colour of the phase tensor ellipses represent the skew angle β (left) and ϕ_{min} (right). For 0.5 km and 1.5 km the phase tensor ellipses are almost all nearly circular and therefore indicate a 1D resistivity structure in shallow depth

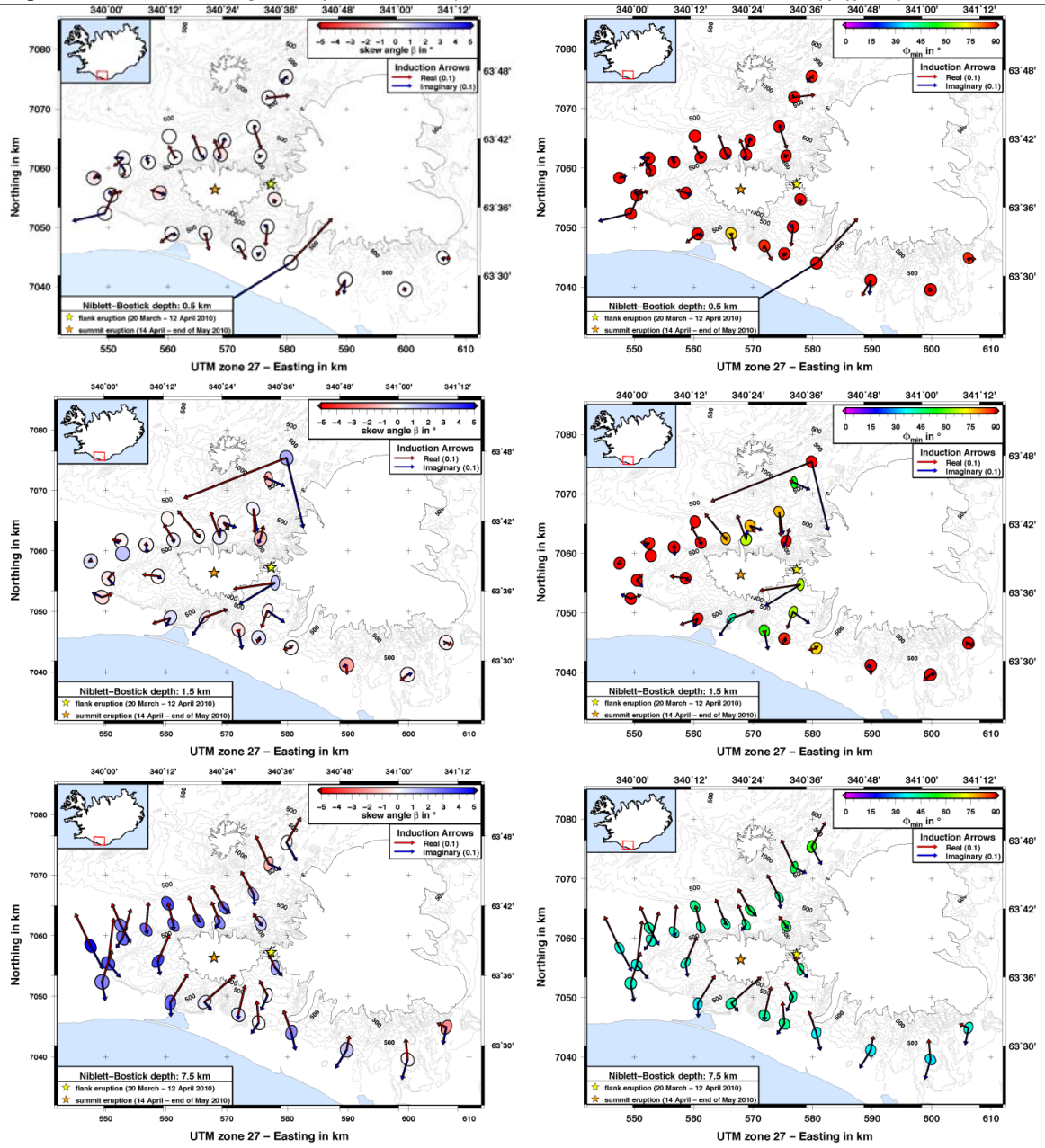

Figure 3: Maps of phase tensor ellipses and induction arrows. For three different depths (0.5, 1.5 and 7.5 km) the real (red) and imaginary (blue) induction arrows are plotted, the arrow length in the legend represents a value of 0.1. The colour of phase tensor ellipses (axes normalised by ϕ_{max}) indicates (left) the skew angle β and (right) ϕ_{min}, respectively. (Note, that the comparable large induction arrow estimates at some sites are not very reliable values as the induction arrows for these sites and these periods range, e.g., in the MT dead-band, scatter a lot.)

(conform with the statement above regarding the first three decades of the response curves in Figure 2). For 7.5 km most phase tensor ellipses are elongated indicating a more complex structure than 1D. The skew angles β are relatively small for all depth and the induction arrow lengths are very short, both indicators for low dimensionality. Large ϕ_{min} values at 0.5 km depth indicate an overall increasing conductivity with depth for the whole survey area. At 1.5 km the sites close to the eruption sites show

moderate ϕ_{min} values (i.e., less strong decrease in resistivity) while all other sites still require a strong decrease in resistivity. At greater depth (7.5 km), the ϕ_{min} values suggest rather constant resistivities or a slight increase. For shallow depth the real induction arrows (red) point away from the Eyjafjallajökull indicating a more conductive structure there compared to the surrounding. At greater depth almost all real induction arrows point away from the Atlantic Ocean. The Icelandic continental shelf has a shallow bathymetry (< 100 m) for the first few kilometres off the coast line, therefore the coast effect only affects long periods/greater depths (see also Figure 2).

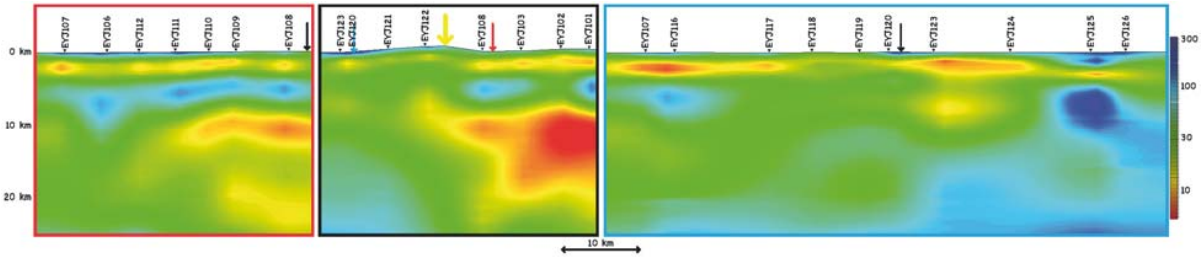

Figure 4: Cross-sections of three profiles. Cross-sections are grids (interpolation radius 3, spline weight 0, smoothing factor 4) of Occam 1D models of the invariants. The coloured boxes indicate where the profiles are located (dashed line of same colour on map in Figure 1) and intersections with other profiles are indicated by an arrow of the same colour. The yellow arrow is the flank eruption location projected onto the profile.

The above suggests that a 1D approach is valid to gain a first impression of the near surface resistivity structures. Therefore, the invariants of the MT data, i.e., geometric mean of resistivities ρ_{xy} and ρ_{yx} and arithmetic mean of phases ϕ_{xy} and ϕ_{yx}, were used to calculate 1D Occam models (Constable et al., 1987). The inversion was ran for maximum 10 iterations using 45 layers with depth limits set to 100 m (top) and 100 km (bottom). Figure 2 shows the resistivity-depth profile obtained for the example site. Such resistivity-depth profiles were calculated for all sites and most show (as in Figure 2) two conductive layers – one at about 1 – 3 km and the other one at about 10 km below surface. Figure 4 shows cross-sections of three profiles (marked by coloured dashed lines in Figure 1) along which the 1D Occam model were smoothly gridded. These cross-sections show also a shallow conductor nearly everywhere, presumably reflecting hydrothermal alteration minerals and, in some parts, a dominant second conductor below 10 km. Previous MT work in Iceland (e.g., Beblo & Björnsson, 1978; Hersir et al., 1984; Eysteinsson & Hermance, 1985) repeatedly showed a conductor in about 10 – 12 km depth nearly everywhere beneath Iceland. The conductive layer was initially interpreted to be due to partial melt in the crust and is still believed to be connected to melt, at least below some parts of the island. However, strong arguments against the presence of a considerable amount of partial melt at this depth interval have been put forward, based on a study of the attenuation of seismic waves (Menke et al., 1995) and later, Kaban et al. (2002) also concluded that considerable melt within the lower crust of Iceland is unlikely. In a recent interpretation of resistivity data from the high temperature area Hengill, SW Iceland the deep conductors are believed to reflect dikes and magma

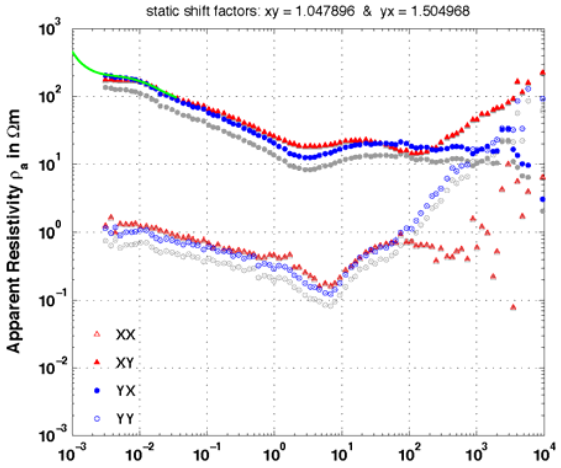

Figure 5: Apparent resistivity curves of an example site. The grey symbols represent the original data whereas the coloured are the data corrected by the static shift factors specified above based on the TEM data (green line).

intrusions and the conductive layer proposed to be due to magmatic brines trapped in ductile intrusive rocks (Árnason et al., 2010). The geological/geophysical reason of the deep-seated high conductive layer is not yet fully understood.

In a next step the obtained TEM data was used to estimate the static shift effects on the original MT data. Displaying TEM data, the apparent resistivity values are usually plotted against time in seconds. To compare the TEM data with the MT data they are plotted using the conversion by Sternberg et al. (1988), where the TEM time is divided by 0.2 to approximate a period on the scale used for MT data. For an example site Figure 5 shows the original apparent resistivity data as grey symbols and the converted TEM curve is represented by the green line. The static shift factors specified above are obtained by calculating the mode (i.e., most frequent value) of the differences in resistivity between the TEM data and each of the XY and YX components of the original MT data. The shift factor XY is applied to the XX and XY MT data and the YX factor to the YX and YY components. The corrected MT data are represented by the coloured symbols. Figure 6 shows a map of all obtained XY and YX static shift factors. Some sites show negligible static shift effects, whereas a few others have more significant effects (mainly only on one E-field direction). Three sites show a shift factor > 1 for one and < 1 for the other direction. These three sites are all located in valleys (especially the south-western one of the three is in an extremely narrow valley). The sites that have a static shift factor close to 2 for one direction are all close to a steep slope. Therefore, the static shift effects found are considered as partly caused by topography. This effect was described by Jiracek (1990).

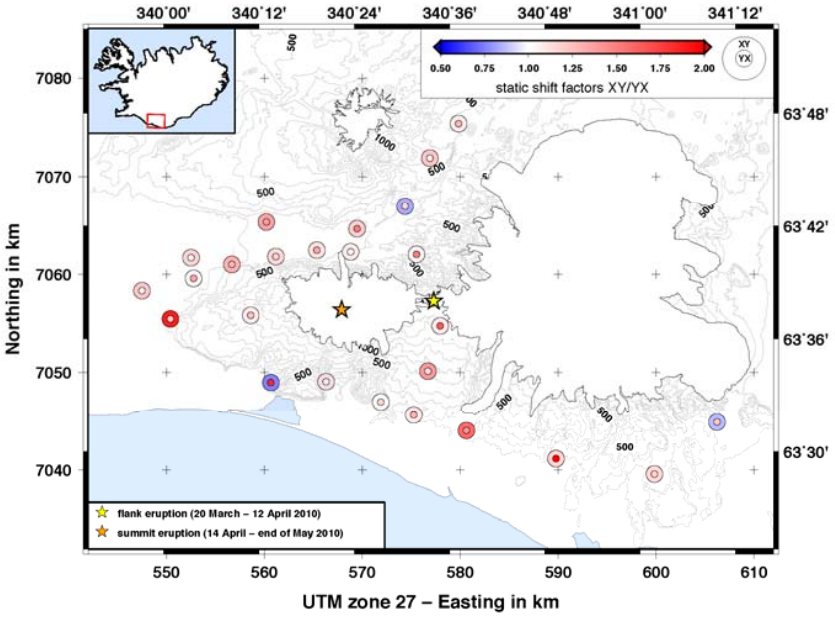

Figure 6: Map showing static shift parameters XY and YX for all sites that have MT and TEM data. The outer circle represents the XY shift factor and the inner dot the YX shift factor.

CONCLUSION & OUTLOOK

The quality of the MT data recorded is very good and all sites show 1D behaviour at short periods. The 1D Occam results (cross-sections as well as resistivity-depth profiles) show two conductive layers; one in approximately 1-3 km depth and one around 10 km depth. The later is conform with many other MT observations across Iceland (e.g., Beblo & Björnsson, 1978; Hersir et al., 1984; Eysteinsson & Hermance, 1985; Árnason et al., 2010). Using TEM data, the MT response curves are corrected for static shift, which is to some extent driven by topography.

The next steps towards a final interpretation will be distortion and strike analysis, 2D and 3D modelling. For interpretation the resistivity models obtained will be compared to other geophysical data

available (e.g., seismicity and GPS data). This study will hopefully be the beginning of a more detailed electromagnetic study of the Eyjafjallajökull and Katla volcanic systems.

ACKNOWLEDGEMENTS

We would like to thank Mark R. Muller, Halldór Örvar Stefánsson, Pálmar Sigurðsson, Sigurbjörn Bogi Jónsson, Alae-Eddine Barkaoui, Anna Wairimu Mwangi, Diego A. Badilla Elizondo, Raymond M. Mwakirani for their indispensable and indefatigable help during the fieldwork.

REFERENCES

Árnadóttir, T., H. Geirsson, S. Hreinsdóttir, S. Jónsson, P. LaFemina, R. Bennett, J. Decriem, A. Holland, S. Metzger, E. Sturkell and T. Villemin (**2008**). *Capturing crustal deformation signals with a new high-rate continuous GPS network in Iceland.* Eos, Transactions, American Geophysical Union 89(53). Fall Meet. Suppl., Abstract G43A-0650

Árnason, K., H. Eysteinsson and G.P. Hersir (**2010)**. *Joint 1D inversion of TEM and MT data and 3D inversion of MT data in the Hengill area, SW Iceland.* Geothermics, vol. 39, 13-34.

Beblo, M., and A. Björnsson (**1978)**. *Magnetotelluric investigation of the lower crust and upper mantle beneath Iceland.* J. Geophys. 45, 1-16.

Björnsson, H., F. Pálsson and M.T. Guðmundsson (**2000**). *Surface and bedrock topography of the Mýrdalsjökull ice cap, Iceland: The Katla caldera, eruption sites and routes of jökulhlaups*. *Jökull* 49, 29-46.

Caldwell, T.W., H.M. Bibby and C. Brown (**2004**). *The magnetotelluric phase tensor*. Geophysical Journal International, 158.

Constable, S.C., R.L. Parker and C.G. Constable (**1987**). *Occam's inversion: A practical algorithm for generating smooth models from electromagnetic sounding data*. Geophysics, 52(3).

Dahm, T. and B. Brandsdóttir (**1997**). *Moment tensors of micro-earthquakes from the Eyjafjallajökull volcano in South Iceland.* Geophysical Journal International, 130*.*

Einarsson, P. and B. Brandsdóttir (**2000**). *Earthquakes in the Myrdalsjökull area, Iceland, 1978–1985: Seasonal correlation and relation to volcanoes*. Jökull 49.

Eysteinsson, H. and J.F. Hermance (**1985**). *Magnetotelluric measurements across the eastern neovolcanic zone in southern Iceland.* Journal of Geophysical Research, 90.

Guđmundsson, M.T., P. Högnadóttir, A.B. Kristinsson and S. Gudbjörnsson (**2007**). *Geothermal activity in the subglacial Katla caldera, Iceland, 1999–2005, studied with radar altimetry*. Annals of Glaciology 45.

Guđmundsson, Ó., B. Brandsdóttir, W. Menke, and G.E. Sigvaldason (**1994**). *The crustal magma chamber of the Katla volcano in South Iceland revealed by 2-D seismic undershooting*. Geophysical Journal International, 119.

Hersir, G.P., A. Björnsson and L.B. Pedersen (**1984)**. *Magnetotelluric survey across the active spreading zone in southwest Iceland.* Journal Volc. Geothermal. Res. 20, 253-265.

Hooper, A., R. Pedersen and F. Sigmundsson (**2009**). *Constraints on magma intrusion at Eyjafjallajökull and Katla volcanoes in Iceland, from time series SAR interferometry*. In: Bean, C.J., Braiden, A.K., Lokmer, I., Martini, F., O'Brien, G.S. (Eds), VOLUME project, EU PF6 (No. 018471). ISBN 978-1- 905254-39-2. VOLUME Project Consortium, Dublin.

Jiracek, G.R. (**1990**). *Near-surface and topographic distortions in electromagnetic induction*. Surveys in Geophysics, 11.

Jones, A.G. and H. Jödicke (**1984**). *Magnetotelluric transfer function estimation improvement by a coherence-based rejection technique*. 54th Ann. Mtg. Soc. of Expl. Geophys., Atlanta, Georiga.

Jones, A.G., A.D. Chave, G. Egbert, D. Auld and K. Bahr (**1989**). *A Comparison of techniques for magnetotelluric response function estimation.* Journal of Geophysical Research (Solid Earth), 94(10).

Jónsson, G. and L. Kristjánsson (**2000**). *Aero-magnetic measurements over Mýrdalsjökull and vicinity*. Jökull 49.

Kaban, M,K, Ó G. Flóvenz and G. Pálmason (**2002)**. *Nature of the crust-mantle transition zone and the thermal state of the upper mantle beneath Iceland from gravity modelling*. Geophys. J. Int. (2002) 149, 281–299.

Larsen, G. (**2000**). *Holocene eruptions within the Katla volcanic system, south Iceland: characteristics and environmental impact*. Jökull 49.

Menke, W., V. Levin and R. Sethi (**1995)**. *Seismic attenuation in the crust at the mid-Atlantic plate boundary in south west Iceland.* Geophys. J. Int. 126, 175-182.

Sigmundsson, F., S. Hreinsdóttir, A. Hopper, T. Árnadóttir, R. Pedersen, M.J. Roberts, N. Óskarsson, A. Auriac, J. Decriem, P. Einarsson, H. Geirsson, M. Hensch, B.G. Ófeigsson, E. Sturkell, H. Sveinbjörnsson and K.L. Feigl (**2010**). *Intrusion triggering of the 2010 Eyjafjallajökull explosive eruption*. Nature, 468.

Sternberg, B.K., J.C. Washburne and L. Pellerin (**1988**). *Correction for static shift in magnetotellurics using transient electromagnetic soundinds*. Geophysics, 53.

Sturkell, E., P. Einarsson, F. Sigmundsson, A. Hooper, B.G. Ófeigsson, H. Geirsson, and H. Ólafsson (**2010**). *Katla and Eyjafjallajökull Volcanoes*. Developments in Quarternary Sciences, 13.

Wiese, H (**1962**). *Geomagnetische Tiefentellurik. II. Die Streichrichtung der Untergrundsstrukturen des elektrischen Widerstandes, erschlossen aus geomagnetischen Variationen*. Geofis. Pura Appl., 52.